A Thesis

On

Synthesis and Characterisation of Magnetic Fluids

Submitted in the partial fulfillment of requirement for the Award of

Degree of Master of Technology (M. Tech)

In

MATERIALS AND METALLURGICAL ENGINEERING

Submitted by

Puneet Moudgil
(Roll No. : 601002002)

Under the Supervision of

Dr. Bhupendrakumar Chudasama
Assistant Professor

School of Physics and Materials Science
Thapar University
Patiala – 147004
INDIA

July 2012

Dedicated to my parents and well wishers

Certificate

This is to certify that the report entitled **"Synthesis and Characterisation of Magnetic Fluids" submitted by Puneet Moudgil, Roll no. 601002002,** in the partial fulfillment of the requirement for the Award of the Degree of M.Tech (Materials and metallurgical Engineering) from the School of Physics & Materials Science, Thapar University, Patiala, is a record of candidate's own work, carried out by her under my supervision. The matter embodied in this report is one of the candidate's own record and not submitted to any other University in any part or full form for the award of such kind of degree.

Dr. Bhupendrakumar Chudasama
Assistant Professor & Supervisor
School of Physics and Materials Science
Thapar University, Patiala

Countersigned by:

Dr. Kulvir Singh
Associate Professor and Head
School of physics and materials science
Thapar University, Patiala
Punjab

(Dr. S.K. Mohapatra)
Dean, Academic Affairs
Thapar University, Patiala
Punjab

Acknowledgment

It gives me profound pleasure to record my heartfelt gratitude to my erudite and revered guide Dr. Bhupendrakumar Chudasama Assistant Professor, School of Physics and Materials Science, for his sense of direction, meticulous efforts, for the completion of my work. I am much indebted for his benevolent help, appreciation, encouragement, enlightens and co-operation.

I shall be failing in my duties if I do not express my deep sense of gratitude towards Dr. Kulvir Singh, Associate Professor& Head, School of Physics and Materials Science, who has been a constant source of inspiration, encouragement, supporting for me throughout my studies here.

I would like to specifically thank Dr. O. P. Pandey, Senior Professor, Dr. N. K. Verma, senior Professor and Dr. Puneet Sharma, Assistant professor, School of Physics and Materials Science for their generous help, encouragement and good wishes.

I express my cordial thanks to Dr. Nidhi Andhariya, DSKPDF *for her timely help, co-operation, encouragement, and useful discussions. I wish to express my heartfelt thanks to research scholars, Miss Chandni, Miss Samita, Mr. Satwinder Singh for their ever-available guidance and indispensable comments, which helped me to develop and shape this study in the present form.*

I owe my sincere thanks to Mr. Purushotam Kumar Singh for helping me during the course of my work and all the staff members of School of Physics and Materials Science for their support and encouragement.

I would also like to extend my love and thanks to my friends who have always been my one of the biggest supporters. Finally, I would like to express my deepest gratitude and love to my parents, without whom I am nothing, for providing me great opportunities, everlasting support, big encouragement and lots of love.

July, 2012

Puneet Moudgil

(PUNEET MOUDGIL)

ABSTRACT

The unusual magnetic properties exhibited by nanoparticles and their promising technological applications have attracted much interest in recent years. The Fe_3O_4 nanoparticles are used in the preparation of biocompatible and temperature sensitive magnetic fluids for variety of applications in biomedicine and engineering. The aim of the present thesis is to prepare highly stable water and automobile oil based magnetic fluids for medicinal and engineering applications, respectively.

This report begins with a detailed description of magnetic fluids and their important applications in chapter 1.Chapter 2 deals with relevant literature review to understand the state of art in the field. The detail methodology of synthesis of nanoparticles and water & oil based magnetic fluids along with various characterization techniques are incorporated in chapter 3. In chapter 4, we have analysed the results obtained from various tests of nanoparticles. Formation of single-phase Fe_3O_4 nanoparticles at low temperature was confirmed by XRD. It was confirmed from TEM analysis that nanoparticles have near spherical morphology. Magnetization measurement reveals that as the applied magnetic fled increases the saturation magnetization of the sample increases. Both, water and oil based magnetic fluids contain superparamagnetic iron oxide nanoparticles with moderately high saturation magnetization.

Contents

List of Figures/Table

Contents

List of tables

Chapter 1

INTRODUCTION

1.1 Magnetic fluids

Ferrofluids or magnetic fluids are stable colloidal homogeneous suspensions of magnetic nanoparticles (around 10 nm in diameter) in an appropriate carrier (aqueous or non-aqueous) liquid. They are superparamagnetic because they are attracted by a magnetic field but retain no residual magnetism after the field is removed. Due to their small size and superparamagnetic behaviour, ferrofluids have been extensively used in several technological and biomedical applications. Iron oxide nanoparticles are generally used as magnetic particles in ferrofluids due to their high saturation magnetization and high magnetic susceptibility [1].

1.2 Components of magnetic fuids: The composition of a typical ferrofluid is about 5% magnetic solids, 10% surfactant and 85% base liquid, by volume.

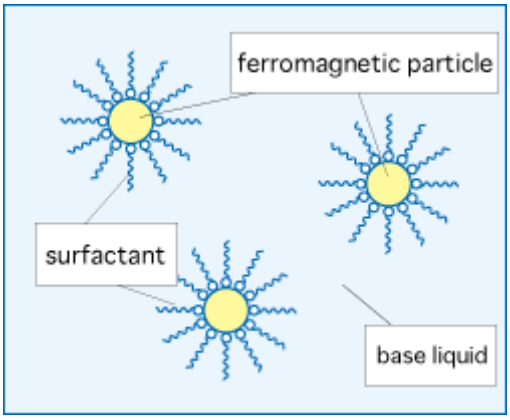

Figure 1.1 Components of magnetic fluids

1.2.1 Magnetic particles: Typically ferrofluids consist of 5% magnetic nanoparticles such as magnetite or composite ferrite. Ferrofluids are composed of nanoscale particles (diameter usually 10 nanometres or less) of magnetite, hematite or some other magnetic compound. This is small enough for thermal agitation to disperse them evenly within a carrier fluid, and for them to contribute to the overall magnetic response of the fluid. When a ferrofluid is subjected to a magnetic field, in order that the colloidal suspension remains stable the magnetic particles generally have to be of approximately 10 nm in diameter. Particles of this size, whether they are ferrite or metal, possess a single magnetic domain only, i.e., the individual particles are in a permanent state of saturation magnetization. Thus a strong long-

range magnetostatic attraction exists between individual particles, the result of which would lead to agglomeration of the particles and subsequent sedimentation [2].

1.2.2 Surfactant: The surfactant coats the ferro/ferri magnetic particles, in order to make colloidal suspension stable. To achieve the repulsive mechanism, the particles can either be coated by a surfactant (surface active material) to produce an entropic repulsion, or the surface of the particles can be charged thereby producing an electrostatic repulsion. Oleic acid is one of the most widely used surfactants. It is generally 10% by volume. The binding of oleic acid with magnetic particles is schematically presented in figure 1.2.

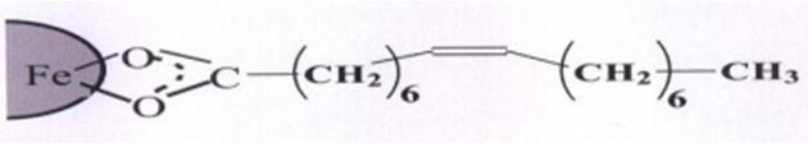

Figure 1.2 Binding of oleic acid with magnetic particles

1.2.3 Base liquid

The carrier liquid may be aqueous or non-aqueous. For engineering applications synthetic or mineral oils are preferred while for biomedical applications water is used. It generally occupies 85% of the fluid volume.

1.3 Types of surfactants

1.3.1 Anionic Surfactant

Anionic Surfactants are dissociated in water in an amphiphilic anion, and a cation, which is in general an alkaline metal (Na+, K+) or a quaternary ammonium. They are the most commonly used surfactants. They include alkylbenzene sulfonates (detergents), (fatty acid) soaps, lauryl sulfate (foaming agent), di-alkyl sulfosuccinate (wetting agent), Lignosulfonates (dispersants) etc. [4].

1.3.2 Cationic Surfactants

These are dissociated in water into an amphiphilic cation and an anion, most often of the halogen type. A very large proportion of this class corresponds to nitrogen compounds such as fatty amine salts and quaternary ammoniums, with one or several long chain of the alkyl

type, often coming from natural fatty acids. These surfactants are in general more expensive than anionics, because of the high pressure hydrogenation reaction to be carried out during their synthesis [5].

1.3.3 Non-ionic Surfactants

They do not ionize in aqueous solution, because their hydrophilic group is of a non-dissociable type, such as alcohol, phenol, ether, ester, or amide. A large proportion of these non-ionic surfactants are made hydrophilic by the presence of a polyethylene glycol chain, obtained by the polycondensation of ethylene oxide. They are called polyethoxyled non-ionic [6].

1.4 Based on the type of surfactants, magnetic fluids are classified into two main groups:

1) Surfacted ferrofluids

2) Ionic ferrofluid

Surfacted ferrofluids

Surfacted ferrofluids are formed by magnetic particles coated with surfactant agents (amphiphilic molecules, as oleic acid and aerosol sodium di-2ethylhexyl-sulfosuccinate) in order to prevent their aggregation.Steric repulsion between particles acts as a physical barrier that keeps particles in the solution and stabilizes the colloid.

If the particles are dispersed in a nonpolar medium, as oil, one layer of surfactant is needed to form an external hydrophobic layer. The polar head of the surfactant is attached to the surface of the particles and the carbonic chain is in contact with the fluid carrier. On the other hand, if the particles are dispersed in a polar medium, as water, a double surfactation of the particles is needed to form a hydrophilic layer around them. The polar heads of surfactant molecules can be cationic, anionic or nonionic. In Figure 1.3 the sketches of an oil based (Figure 1.3a) and water-based (Figure 1.3b) ferrofluid grainsparticles are presented [7].

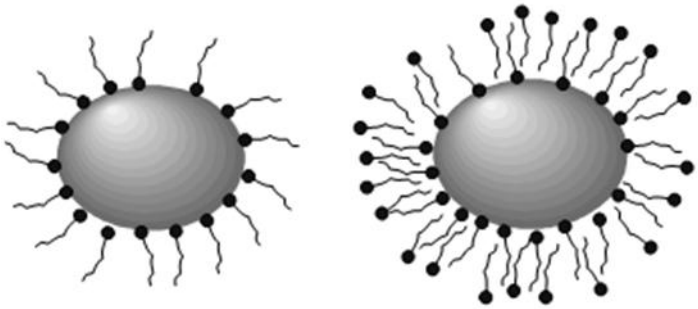

(a) (b)

Figure 1.3 Surfacted ferrofluids grains: (a) Single-layered grains (b) Double-layered grains

Ionic ferrofluids

In ionic ferrofluids, nanoparticles are electrically charged to keep the colloidal system stable. Usually, the liquid carrier is water and the pH of the solution can vary from 2 to 12 depending on the sign of the surface charge of the particles. Acid ionic ferrofluid (pH < 7) have positively charged ferrofluid particles, and alkaline ionic ferrofluid (pH > 7) have negatively charged particles. The surface charged density of the particles is typically of the order of 10 μC /cm^{2}and it is a function of the solution pH [8].

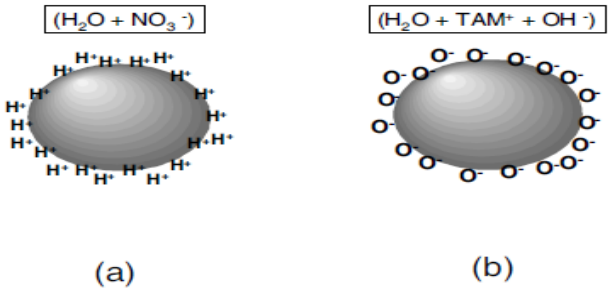

Figure 1.4 Sketch of ionic ferrofluid particles. The counterions and the water molecules are also indicated: a) acid ferrofluid particle; b) alkaline ferrofluid particle, TAM^+OH^- is the tetra methyl ammonium hydroxide.

1.5 Properties of magnetic fluids

1.5.1 Spiking phenomenon

Figure 1.5 shows a phenomenon that occurs when ferrofluid is placed in a container and a magnet is placed under the container. The magnetic force acting on the surface of the

ferrofluid produces spikes which look like large nails sticking out of the surface. Therefore, this phenomenon is called spiking.

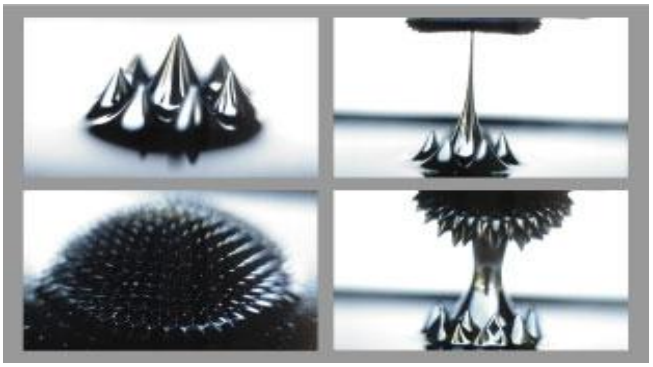

Figure 1.5 Spiking in magnetic fluid

1.5.2 Rheological properties of magnetic fluids

An increase of viscosity in magnetic fluids generated by the influence of the field can easily be understood on the basis of a simple microscopical model. As shown in Fig. 1.6 the shear flow will cause a rotation of the magnetic particles due to the difference in viscous friction forces acting at opposite radial positions. If a magnetic field is applied to the system, the magnetic moment of the particle will try to align with the field direction. In a situation where the field is perpendicular to the vorticity of the flow, i.e. to the axis of rotation of the particles, the rotation of the particles provided by the viscous torque in the fluid will force a disalignment of the magnetic moment from the field direction as shown in figure 1.6a. This disalignment itself will give rise to a magnetic torque counteracting the viscous torque. The existence of two opposing torques in the described situation results in a hindrance of the free rotation of the magnetic particles in the flow which generates macroscopically an increase of the fluid's viscosity. As an interesting additional aspect of this field dependent viscosity change one should note that the effect shows a pronounced anisotropy. If field and vorticity are parallel the effect vanishes since the alignment of the magnetic moment of the particle with the field direction is not disturbed by the particle's rotation as shown in figure 1.6b [9].

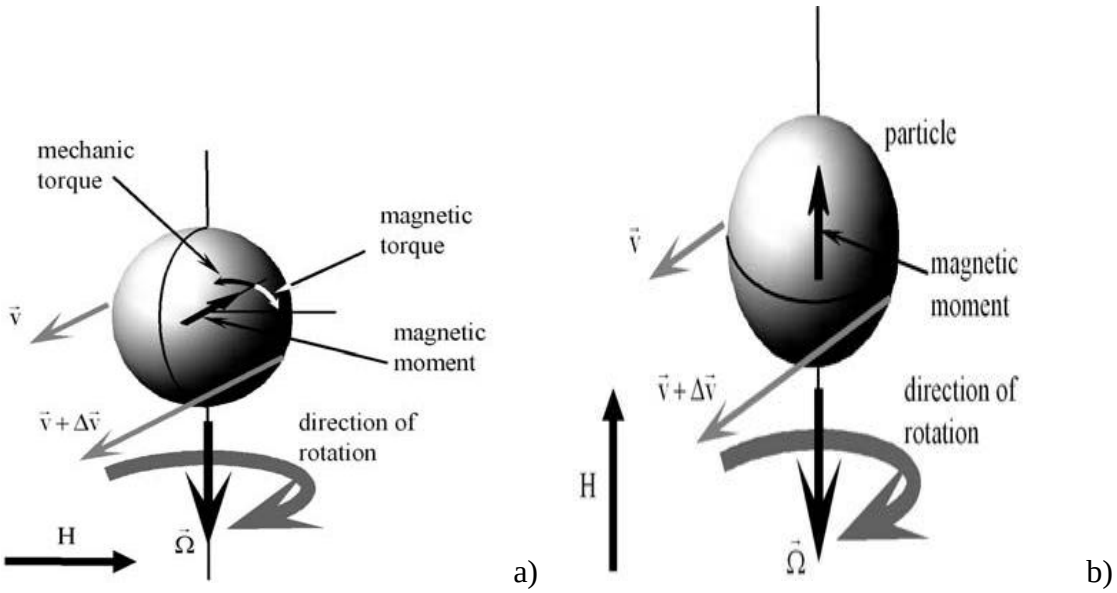

Figure 1.6 General microscopical model for the explanation of the appearance of a field dependent increase of viscosity in a diluted ferrofluid.

1.6 Applications of ferrofluids

1.6.1 Technological Applications

1) Dynamic sealing

In the hard disks of computers, these have to be operated in a hermetically closed box because any grain of powder or even smoke may spoil the reading and writing process. Therefore it is necessary to seal hermetically the hole through which the axle passes. This is achieved by making the hole inside a magnet (see Fig. 1.7) and the shaft made of soft magnetic material. A groove in the shaft is filled up with ferrofluid, which is kept in place by the magnetic field, obstructing the passage of any impurity, but leaving the axle free to rotate, because the obstructing material is liquid [10].

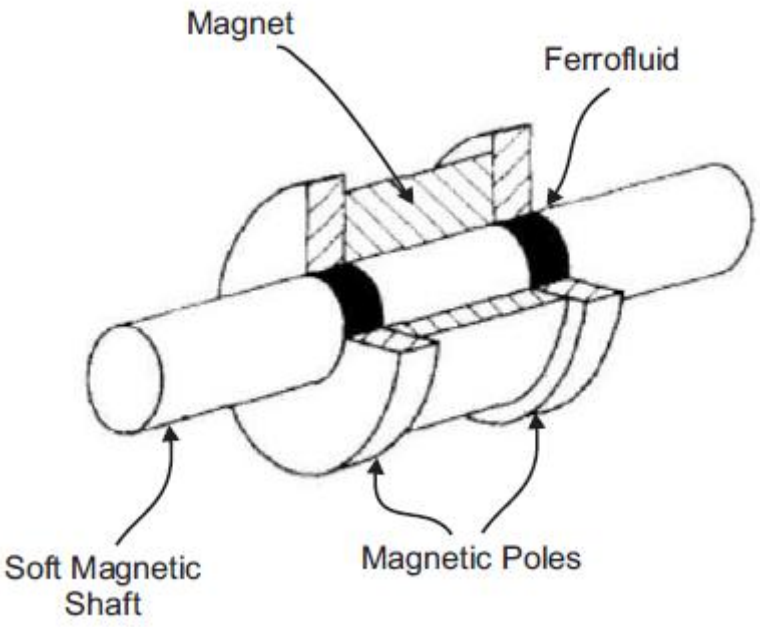

Figure 1.7 Dynamic seal

(ii) Heat dissipation: One way of extracting heat from equipment which heats up by functioning, and so keeping it at appropriate temperature, is by using a good heat conductor which connects the equipment to some mass which has much bigger heat capacity and, much bigger open surface to dissipate heat. In some cases the good heat conductor must not be a solid, because it would block the equipment's operation because it will vibrate. One way to achieve the desired goal is by using a ferrofluid as heat conductor. A non-magnetic liquid would flow away from the place where it is supposed to operate. A good example is a loudspeaker, whose coil heats up by functioning and the ferrofluid is kept in place by the magnetic field of the magnet which is fixed on the loudspeaker's horn. Now a day's most of the high power loudspeakers are equipped with ferrofluid. The presence of the fluid around the coil improves also the quality of the speaker because it damps unwanted resonances which would produce a very unpleasant noise [11].

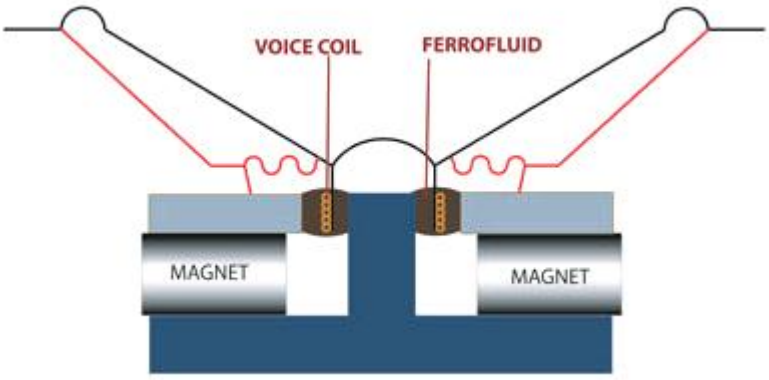

Figure 1.8 Speaker with ferrofluids in air gap

(iii) Inertial and viscous damper

The magnetic fluids are used also as dampers in loudspeakers. A more direct use for damping unwanted vibrations is associated to their use as inertial and viscous dampers for motors, mainly stepper motors. For this purpose we can use the property of magnetic fluids that, whose mass density is bigger than that of the fluid, floating in it, with part of its volume above the liquid's surface. This is because the magnetic field gradient pulls the magnetic fluid to the region under the immersed pole of the magnet, causing a pressure (magnetic pressure) which pushes the magnet up. The equilibrium is established when the magnet's weight is counterbalanced by this magnetic pressure and the hydrostatic pressure. Even a non-magnetic body can levitate if there is a magnetic field gradient applied on the ferrofluid, which causes a magnetic pressure gradient in the fluid. A stepper motor operated at its natural frequency may experience excessive settling time, vibration and acoustic noise. A damper absorbs the unwanted vibration by a shearing effect which produces a torque that opposes the oscillatory motion. The damper has a non-magnetic housing which attaches to the motor shaft. Inside the housing is an inertial mass which levitates on ferrofluid, thus eliminating the need for bearings to support the mass [12].

1.6.2 Material recycling

Ferrofluid has a unique property; applying magnetic field to the ferrofluid will increase its apparent density. This physical characteristic creates the ability to separate objects of different density through floatation or sinking. Ferrofluids have been used for years in material separation processes in the mining industries.

1.6.3 Biomedical Applications

(i) Magnetic drug targeting: Localizability of a portion of ferrofluid by a magnetic field, associated with the fact that any liquid may be turned into a magnetic fluid, offers very interesting applicability in medicine. Much work has been done to bind ferrofluids with drugs for chemotherapy. The idea is such a ferrofluid bounded drug is injected in a cancer tumour and there it is kept by a suitably focused magnetic field, where it has a very intense and localized action.

The amount of drug necessary is much less than what would be necessary if it is dispersed in the whole body. When the magnetic field is turned off the drug will disperse in the body, but, since the total amount is very small, there will be practically no side effects [13].

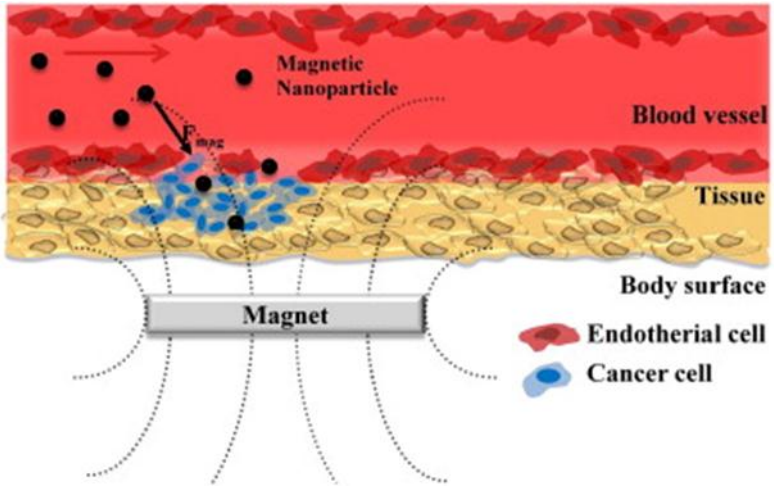

Figure 1.9 Hypothetical magnetic drug delivery system shown in cross-section: a magnet is placed outside the body in order that its magnetic field gradient might capture magnetic carriers flowing in the circulatory system.

(ii) Magnetic cell separation: In biomedicine it is often advantageous to separate out specific biological entities from their native environment. Magnetic separation using biocompatible nanoparticles is one way to achieve this. It is a two-step process, involving:

(1) The tagging or labelling of the desired biological entity with magnetic material.

(2) The separating out of these tagged entities via a fluid-based magnetic separation device.

Tagging is made possible through chemical modification of the surface of the magnetic nanoparticles, usually by coating with biocompatible molecules such as dextran, polyvinyl alcohol (PVA) and phosopholipids. The magnetically labelled material is separated from its native solution by passing the fluid mixture through a region in which there is a magnetic field gradient which can immobilize the tagged material via the magnetic force.

Magnetic separator design can be as simple as the application and removal of a permanent magnet to the wall of a test tube to cause aggregation, followed by removal of the supernatant (Figure 1.10 (a)). A typical way to achieve this is to loosely pack a flow column with a magnetisable matrix of wire (e.g. steel wool) or beads and to pump the magnetically tagged fluid through the column while a field is applied (Figure 1.10(b)) [14].

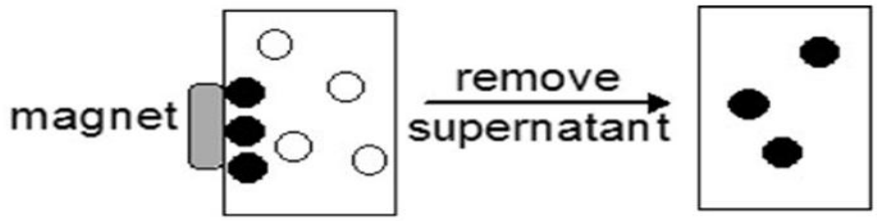

Figure 1.10 (a) A magnet is attached to the container wall of a solution of magnetically tagged (•) and unwanted (◦) biomaterials. The tagged particles are gathered by the magnet, and the unwanted supernatant solution is removed.

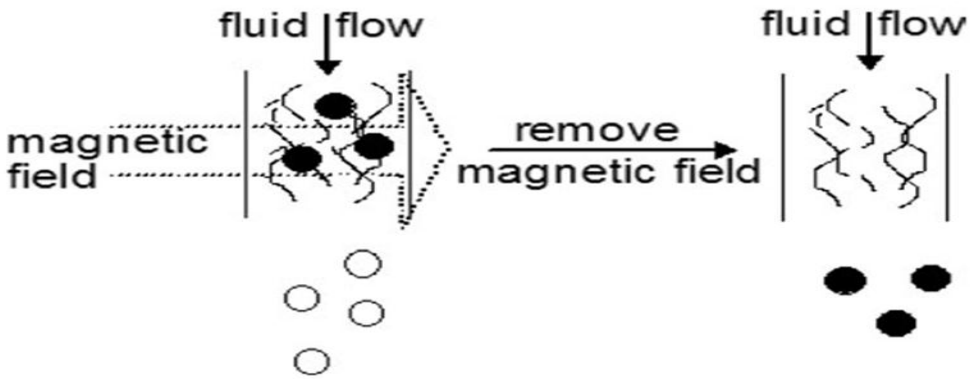

Figure 1.10 (b) A solution containing tagged and unwanted biomaterials flows continuously through a region of strong magnetic field gradient, often provided by packing the column with steel wool, which captures the tagged particles. Thereafter the tagged articles are recovered by removing the field and flushing through with water.

(iii) Hyperthermia: The property of ferrofluids of absorbing electromagnetic energy at a frequency that is different from the frequency at which water absorbs energy allows one to

heat up a localized portion of a living body, where ferrofluid has been injected, for example a tumour, without heating at the same time the surrounding parts of the body. A number of experiments, healing cancer tumours in rats and rabbits by this technique have been reported during the last few years. In the year of 2004 a new important step was given in this direction Humans has had their cancer tumours successfully treated by magnetic fluid hyperthermia [15].

(iv) Contrast enhancement for Magnetic Resonance Imaging

MRI has been one of the most powerful diagnosis techniques used in medicine in recent years. Its ability to distinguish between different tissues relies on the different relaxation times T of the proton's magnetic moments when it is inside different ambients. Frequently, however, the differences are not strong enough to render well resolved images. If magnetic particles from a biocompatible ferrofluid are selectively absorbed by some kind of tissue, this will become very clearly visible by MRI. Moreover, different tissues uptake different amounts of the magnetic particles, having therefore different values of T and distinguishable images. Dextran coated iron oxides are biocompatible and are excreted via the liver after the treatment. They are selectively taken up by the reticuloendothelial system. This is important because tumour cells do not have the effective reticuloendothelial system of healthy cells, so healthy that their relaxation time is not altered by the contrast agent, which makes them distinguishable from the surrounding cells [16].

1.6.4 Engineering Application

(i) Transformer cooling

Ferrofluids have been shown to provide both thermal and dielectric benefits to transformers. Ferrofluid can be utilized to improve cooling by enhancing fluid circulation within transformer windings. Ferrofluid can also be applied to increase transformer capacity to withstand lightning impulses, while also minimizing the effect of moisture on typical insulating fluids. The benefits of ferrofluid may be utilized to design smaller, more efficient new transformers, or to extend the life or loading capability of existing units. Ferrofluids have been shown to provide higher capacity to sustain overvoltage, and present better resilience at degradation in time due to the humidity as compared to classic oils [17].

Figure 1.11 Phased transformers with ferrofluid coolant system

(ii) Quiet Solenoids

The introduction of a ferrofluid into a solenoid dramatically reduces the noise level of certain equipment, such as home care kidney dialysis machines. This in turn reduces the need for noise suppression insulation, allowing a more cost effective and simpler design that is more portable. In addition to the obvious benefits of quieter operation and portability, the ferrofluid-based solenoids make the equipment more reliable.

(iii) Sensors & Switches

The unique properties of magnetic fluid make it a feasible technology for some sensor and switch applications. The use of ferrofluid may enhance the motion sensitivity in some sensing applications. Ferrofluid application includes inclinometers, accelerometers and flow meters, tilt, vibration, pressure and level sensors, and various switches [18].

Chapter 2

LITERATURE REVIEW

There are many methods for the preparation of magnetite nanoparticles. Some of the methods are:

2.1 Ball –milling

2.2 Hydrothermal precipitation

2.3 In-situ method

2.4 Solid State Chemical Reaction Method

2.5 Micro-emulsion method

2.6 Co-precipitation method

2.7 Thermal decomposition method

2.1 Ball-milling

V. M. Chakka et al. [19] in 2006 prepared nanoparticles of Fe, Co, FeCo, SmCo, and NdFeB by ball milling in the presence of surfactants and organic carrier liquid. It was observed that the nanoparticles prepared by milling Fe and FeCo powders were close to spherical in their shapes, whereas those of Co, SmCo, and Nd–Fe–B showed elongated rod shapes. The nanoparticles showed superparamagnetic behavior at room temperature, except for the SmCo nanoparticles that were ferromagnetic. Magnetic measurements at room temperature were performed using an alternating gradient magnetometer with measuring field up to 14 kOe, and at 5 K using a superconducting quantum interference device SQUID with measuring field up to 70 kOe. Structural and morphological characterizations were performed using transmission electron microscope TEM, and X-ray diffractometer. Compositional characterizations were performed using energy dispersive x-ray and inductively coupled plasma.

2.2 Hydrothermal precipitation

Shouhu Xuan et al [19] in 2006 prepared water-soluble magnetite nanoparticles by a hydrothermal method. In this work, hydrated ferric salt was employed as a single iron precursor and ascorbic acid as a reducing agent to synthesize superparamagnetic Fe_3O_4 nanocrystals, which capped with $C_6H_6O_6$ (the oxidation state of ascorbic acid). The final product was characterized with X-ray powder diffraction (XRD), transmission electron microscope (TEM), Fourier Transform, Infrared and X-ray photoelectron spectroscopy. The experimental results reveal that ascorbic acid not only serves as a reducing reagent for the reaction, but also the oxidation state of ascorbic acid involves surface coordination which renders the magnetite nanocrystals water soluble and the colloidal solution stable. Those particles were only several nanometers long, as shown by TEM. They show the typical behavior of superparamagnets at room temperature.

2.3 In-situ method

Nashaat N. Nassar et al [20] presented a novel approach for the preparation of iron oxide nanoparticles in w/o microemulsions. $FeCl_3$ bulk powder was subjected to the action of microemulsions formed with sodium bis (2-ethylhexyl) sulfosuccinate (AOT), an anionic surfactant. Iron chloride first solubilized into the water pools of the microemulsions, then reacted with sodium hydroxide added to the water pools of the microemulsion to eventually form the iron oxide nanoparticles. This technique served as an in-situ preparation of nanoparticle catalysts which find applications in the in-situ heavy oil upgrading. The nanoparticle morphology and size distribution was determined using the Small Angel X-Ray Scattering, Transmission Electron Microscopy (TEM), and UV spectroscopy by changing concentration of $FeCl_3$.

2.4 Solid State Chemical Reaction Method

Hassan Karami et al. [21] synthesized iron oxide particles by solid state chemical reaction method. The synthesized powders were characterized by XRD, SEM, EDAX and TG-DTA techniques. An average grain size of 10–20 nm for Maghemite and 80–85 nm for Hematite was calculated using XRD line broadening and SEM. The effect of different parameters such as annealing temperature, milling time, Fe^{+3}: Fe^{+2} concentration ratio was investigated on the particle size and phase formation.

2.5 Microemulsion method

Nguyen Thai Ha et al. [22] in 2008 prepared Fe_3O_4 nanoparticles by the microemulsion technique with water as the aqueous phase, n-hexane as the oil phase and Span 80 as the surfactant. The reaction occurred under air, N_2 or high temperature and high pressure atmosphere. Particle size was less than 10 nm measured by SEM which was in agreement with XRD results. Magnetic properties were measured by VSM. The saturation magnetization was 50 emu/g . Functionalization of the particle surface was carried out by using a single layer of oleic acid for hydrophilic surface and double layer of oleic acid and sodium dodecyl sulfate for hydrophilic surface to disperse them in non-aqueous and aqueous solvents, respectively.

2.6 Co-Precipitation method

D. Maity et al. [23] in 2007 worked on the magnetic fluids. The particles have been suspended in non-aqueous and aqueous media by coating the particles with a single layer and a bilayer of oleic acid, respectively. The particle sizes, morphology and the magnetic properties of the particles and the ferrofulids prepared from these particles were reported. The average particle sizes obtained from the TEM micrographs were 14, 10 and 9 nm for the water, kerosene and dodecane-based ferrofluids, respectively, indicating a better dispersion in the non-aqueous media. The specific saturation magnetization value of the oleic-acid-coated particles (53 emu /g) was found to be lower than that for the uncoated particles (63 emu/g).

W. Voit et al. [24] in 2001 worked on the magnetic behaviour of nanosized iron oxide particles coated with different surfactants (sodium oleate, PVA and starch) in a ferrofluid. The superparamagnetic iron oxide particles, synthesized by a controlled co-precipitation technique, were found to contain magnetite (Fe_3O_4) as a main phase with a narrow physical particle size distribution between 6 and 8 nm. The mean effective magnetic size of the particles in different ferrofluid systems were estimated to be around 4-5 nm which was smaller than the physical particle size. On a 10% dilution in the starch coated ferrofluid, there was a decrease in the blocking temperature.

M. Kawashita et al.[25] in 2011 synthesised magnetite nanoparticles (MNPs) with series of size varying from 8 nm to 103 nm by a chemical co-precipitation and an oxidation precipitation method to aim for finding the optimum particle size which has high heating

efficiency in the applied magnetic field (9.6–23.9 kAm^{-1}, 100 kHz). Their in vitro heating efficiencies in agar phantom, at a MNPs concentration of 58mg Fe ml^{-1}, were measured in the applied field. The temperature increase (ΔT) of the agar phantom at 30 s was 9.3 °C for MNPs of 8 nm, exhibiting a high heating efficiency in a field intensity of 9.6 kAm^{-1}.The ΔT of agar was 55 °C for MNPs of 24 nm and 25 °C for MNPs of 8 nm in a field intensity of 23.9 kAm^{-1}. The excellent heating efficiency for MNPs of 24 nm might be a combined effect of relaxation loss and hysteresis loss of the magnetic particles.

Roberto Valenzuela et.al.[26] in 2009 synthesised Superparamagnetic magnetite nanoparticles (mean diameter ∼10 nm) using the co-precipitation route from $Fe^{2+/}Fe^{3+}$ in aqueous solutions (molar ratio 1:2) by adding a base under mechanical stirring at 10,000 rpm. This stirring velocity was found to be suitable for obtaining nanoparticles of this mean size, and a decrease in stirring velocity resulted in a larger size (∼19 nm) and a wider size distribution. At 18,000 rpm, in addition to magnetite, goethite was also synthesized in the form of nanoparticles and nano rods were found. At higher stirring velocities (25,000 rpm), the solution's core temperature increased from 20° to 37 °C, generating a mixture of non-magnetic iron compounds.

2.7 Thermal decomposition method

Maity et.al. [27] in 2008 synthesized Fe_3O_4 nanoparticles by a novel solvent-free thermal decomposition method. Size and morphology of the nanoparticles were determined by TEM while the structure of the nanoparticles was identified by FTIR, XPS and TGA measurements. Magnetic properties of the obtained particles were determined using VSM and SQUID measurement. The particle size of the Fe_3O_4 was tailored by adjusting either reaction temperature or time. When the reaction temperature was increased to 330 °C and the reaction time was extended to 4 h, the average particle size of the obtained nanoparticles was 9 nm, while M_s Value reached 76 emu/g. The Fe_3O_4 nanoparticles showed well-established superparamagnetic properties with the blocking temperature at around 100 K.

Suk Fun Chin et.al. [28] in 2011 synthesised Fe_3O_4 nanoparticles with controllable size and shape by the thermal decomposition method. This method utilized a much cheaper and less toxic iron precursor, iron acetylacetonate (Fe (acac) ^{3}), and environmentally benign and non-toxic polyethylene oxide (PEO) was being used as the solvent and surfactant simultaneously. Fe_3O_4 nanoparticles of controllable size and shape were prepared by manipulating the

synthesis parameters such as precursor concentrations, reaction durations and surfactants. The mean size of Fe_3O_4 nanoparticles was observed by TEM .It was increase with increased concentrations of Fe $(acac)^3$ precursors, which varied between 2 nm to 7 nm as the concentration of Fe $(acac)^3$ was increased from 0.1 mmol to 8 mmol.

. **Chapter 3**

SYNTHESIS AND CHARACTERISATION TECHNIQUES

3.1 Processes for producing nanoparticles

There are two approaches to the synthesis of nanomaterials. They are (i) top-down and (ii) bottom-up process.

3.1.1 Top down process

By this group of techniques bulk materials are broken into nano-sized particles.

Examples:

(1) Ball Milling

(2) CVD

(3) Laser induced gas evaporation method.

(4) Plasma Arcing

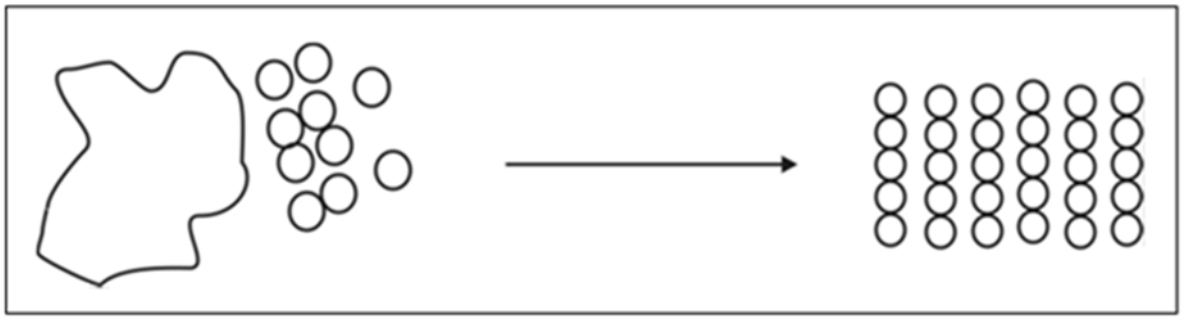

Figure 3.1 Top down process

(1) Ball Milling

Principle: Small hard balls are allowed to rotate inside a container and then it is made to fall on a solid with high force to crush the solid into nanocrystals.

Construction and Working: Hardened steel or tungsten carbide balls are put in a container along with powder of particles of a desired material. The container is closed with tight lids. When the container is rotating around the central axis, the material is forced to press against

the walls. The milling balls impart energy on collision and produce smaller grain size of nano particles. Ball milling is also known as mechanical alloying or crushing [29].

Advantages of Ball Milling

(1) Few mg to several kg of nanoparticle can be synthesized in a short time.

(2) This technique can be operated at large scale.

Applications

(1) Ball milling is useful in preparation of elemental and metal oxide nano crystals like Co, Cr, Al-Fe, Ag-Fe and Fe.

(2) Variety of intermetallic compounds of Ni and Al can be formed.

2) Chemical Vapour Deposition (CVD):

Principle: The reactant particles are mixed with carrier gas and allowed to pass on through the hot solid substrate surface. When the reactant particles and substrate comes in contact, the heat energy initiates the chemical reactions and form nano film on the substrate surface. The by-products of the reactions on the solid surface can be removed by washing.

CVD coatings have following characteristics:

(1) Fine grained

(2) High purity

(3) Harder than similar materials produced using conventional ceramic fabrication processes.

(4) CVD coatings are usually only a few microns thick and are generally deposited at fairly slow rates, usually of the order of a few hundred microns per hour.

CVD Apparatus

A CVD apparatus will consist of several basic components:

(1) Gas delivery system – For the supply of precursors to the reactor chamber.

(2) Reactor chamber – Chamber within which deposition takes place.

(3) Substrate loading mechanism – A system for introducing and removing substrates, mandrels etc.

(4) Energy source – Provide the energy/heat that is required to get the precursors to react/decompose. Resistive Heating, Radio Frequency heating, Lasers etc.

(5) Vacuum system – A system for removal of all other gaseous species other than those required for the reaction/deposition.

(6) Exhaust system – System for removal of volatile by-products from the reaction chamber.

(7) Exhaust treatment systems – In some instances, exhaust gases may not be suitable for release into the atmosphere and may require treatment or conversion to safe/harmless compounds.

(8) Process control equipment – Gauges, controls etc. to monitor process parameters such as pressure, temperature and time. Alarms and safety devices would also be included in this category [30].

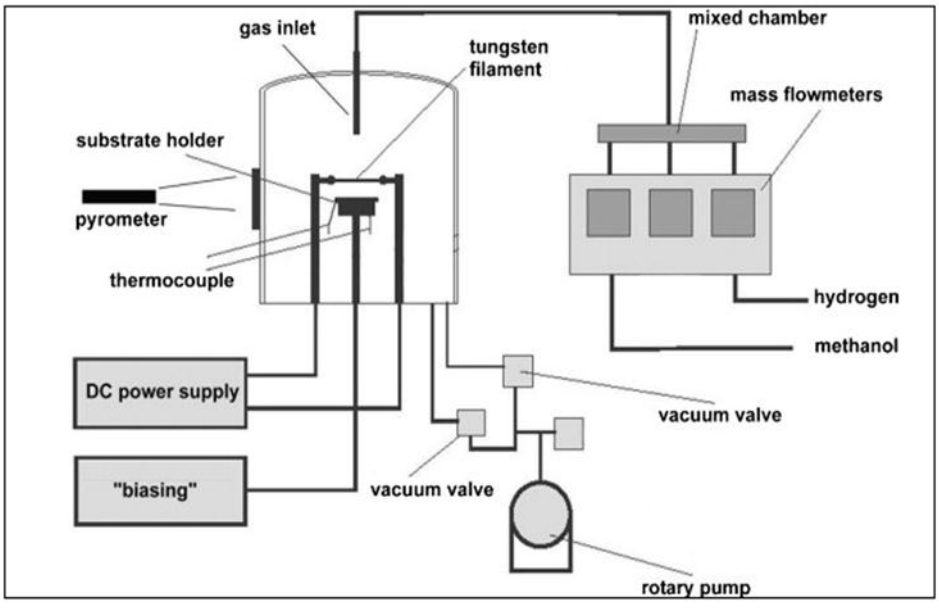

Figure 3.2 Schematic diagram of CVD apparatus

Applications

CVD has applications across a wide range of industries such as:

(1) Coatings – Coatings for a variety of applications such as wear resistance, corrosion resistance, high temperature protection, erosion protection etc.

(2) Semiconductors and related devices – Integrated circuits, sensors and optoelectronic devices.

(3) Dense structural parts – CVD can be used to produce components that are difficult or uneconomical to produce using conventional fabrication techniques. Dense parts produced via CVD are generally thin walled and may be deposited onto a mandrel or former.

(4) Optical Fibres – For telecommunications.

(5) Composites – Preforms can be infiltrated using CVD techniques to produce ceramic matrix composites such as carbon-carbon, carbon-silicon carbide and silicon carbide-silicon carbide composites. This process is sometimes called chemical vapour infiltration or CVI [31].

3) Laser induced gas evaporation method

Instead of combustion of a liquid precursor giving access to oxidic nanoparticles, Kato showed in 1976 that he was able to produce a range of different ultrafine refractory oxides (SiO_2, MgO, Al_2O_3, Fe_3O4, Mg_2SiO_4, $CaTiO_3$ and $MgAl_2O_4$) by the use of a CO_2 laser. The laser was used to vaporize starting material in form of powder or sintered or fused blocks. The vaporized material condensed in an environment of inactive gases and resulted in nanoparticles.

4) Plasma based nanoparticle production

A similar method to laser induced gas evaporation are plasma reactors. In this case plasma delivers the energy necessary to evaporate the starting materials of various types including gases, liquids and solid. At temperatures of around 10,000°C the plasma generates reactive ions and radicals. During the pull-out from the plasma region the temperature of the gas drops and nanoparticles are formed. Plasma based methods have been used to synthesize nanoparticles in form of metal oxides, metals or metal nitrides.

3.1.2 Bottom-up process

Nanomaterials are produced by building of atom by an atom.

Examples:

1. Sol-Gel method

2. Co-precipitation method

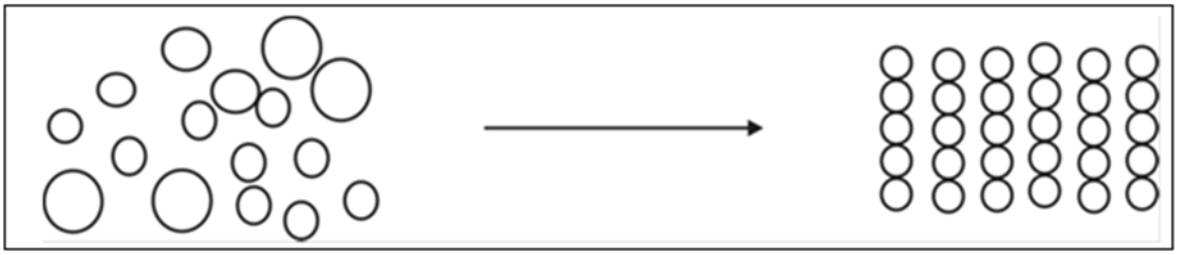

Figure 3.3 Bottom up process

(1) Sol gel process: Sol-gel method is wet-chemical processes for producing porous nanomaterials, ceramic nanostructured polymers as well as oxide nanoparticles. The synthesis takes place under relatively mild conditions and low temperatures. The term sol refers to dispersions of solid particles in the 1-100 nm size range, which are finely distributed in water or organic solvents. In sol-gel processes, material production or deposition takes place from a liquid sol state, which is converted into a solid gel state via a sol-gel transformation. The sol-gel transformation involves a three-dimensional cross-linking of the nanoparticles in the solvent, whereby the gel takes on bulk properties. A controlled heat treatment in air can transform gels into a ceramic oxide material.

To start with, adding organic substances in the sol-gel process produces an organometallic compound from a solution containing an alcoxide (metallic compound of an alcohol, for example with silicon, titanium or aluminium). The pH value of the solution is adjusted with an acid or a base which, as a catalyst, also triggers the transformation of the alcoxide. The subsequent reactions are hydrolysis (splitting of a chemical bond by water) followed by condensation and polymerization (reaction giving rise to many- or long-chained compounds from single chained ones). The particles or the polymer oxide grow as the reaction continues, until a gel is formed. Due to the high porosity of the network, the particles typically have a large surface area, i.e. several hundred square meters per gram. The course of hydrolysis and the poly condensation reaction depend on many factors:

(1) The composition of the initial solution.

(2) The type and amount of catalyst.

(3) Temperature as well as the reactor- and mixing geometry.

For coatings, the alcoxide initial solution of the sol-gel process can be applied on surfaces of any geometry. After the wetting, the build-up of the porous network takes place through gel formation, yielding thicknesses of 50-500 nm. Thicker layers, suitable as membranes for example, are created by repeated wetting and drying. The sol-gel process can also be used to produce fibers. In all cases, gel formation is followed by a drying step.

Advantages of the sol- gel process

(1) The sol - gel method used in the raw material is first dispersed to a solvent to form low viscosity of the solution, therefore, it can in a very short period of time to obtain the uniformity of the molecular level, in the formation of gel, is likely to be between the reactants at the molecular level is evenly mixed.

(2) Easy to carry out the reaction.

(3) The temperature is lower.

Applications of the sol-gel process:

(1) Protective and decorative coatings and electro-optic components can be applied to glass, metal and other types of substrates with these methods.

(2) Powder abrasives, used in a variety of finishing operations, are made using a sol-gel type process.

(3)Another application in research is to entrap biomolecules for biosensors or catalytic purposes [32].

(2) Co-precipitation method (Preparation of magnetic fluids)

Ferrofluids do not exist in nature and are artificially prepared. The earliest method to produce ferrofluids was by grinding micro-sized magnetic particles for several weeks in ball mills in the presence of surfactants, producing a very broad particle size distribution. A more convenient method, which also results in better-defined particles with a much narrower size distribution, is the preparation by precipitation reactions. A well-known example is the

synthesis of magnetite by the addition of a stoichiometric mixture of Fe (II) and Fe (III) salts to an alkali solution [33].

Chemical reaction:

$8OH^- + 2Fe^{3+} + Fe^{2+} \rightarrow Fe_3O_4 + 4H_2O$

Aqueous dispersions of iron oxide particles are stabilized by a hydrophilic double layer of surfactants or by charge (due to acid-base reactions at the surface or specific adsorption of ions). The first (water-based) ferrofluid was synthesized in 1938 by Elmore (via the ball-mill procedure), but extensive research on ferrofluids started around 1960 by NASA. They developed the synthesis of oil-based ferrofluids stabilized by surfactants that are still used today. This method is followed because of following reasons [34].

1) Simple and rapid preparation.

2) Easy control of particle size and composition.

3) Various possibilities to modify the particle surface state and overall homogeneity.

4) It is inexpensive.

5) Time saving.

6) Processed at much lower temperature.

1) Synthesis of oil based magnetic fluid

Materials required: $FeSO_4.7H_2O$, $FeCl_3.6H_2O$, NaOH, Distilled water, Oleic acid etc.

Chemical reaction:

$FeSO_4.7H_2O + 2FeCl_3.6H_2O + 8NaOH \rightarrow Fe_3O_4 + 6NaCl + Na_2(SO_4) + 23H_2O$

PROCEDURE

(1) 27.8 gm. of $FeSO_4.7H_2O$ was dissolved in 100 ml water, 54 gm. of $FeCl_3.6H_2O$ was dissolved in 100 ml and 64 gm. of NaOH was dissolved in 200 ml water.

(2) Solutions of iron sulphate and iron chloride were mixed together.

(3) Dilute hydrochloric acid was added till pH of the solution falls to 1.5.

(4) All the solutions were added .pH increased up to 10.5.

(5) Solution was stirred for 20 minutes.

(6) Then solution was decanted 4 times with the help of permanent magnet with the help of distilled water.

(7) Hydrocarbon based ferrofluids were prepared from the precipitated fine particles directly by using oleic acid as the surfactant Oleic acid was converted to sodium oleate and was transferred to the beaker 3.

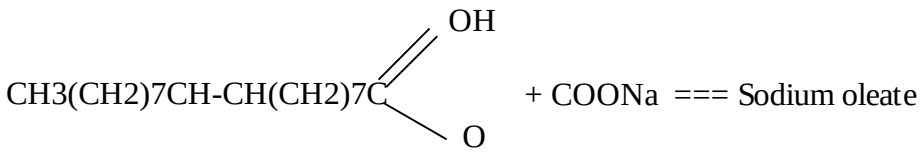

(8) Stirring was continued for 1 hour and coating of surfactant was carried out at 93 °C.

(9) To coagulate the oleic acid-coated particles, dilute HCl was added until the pH of the solution falls below 5.

(10) After decantation, the resulting product was washed many times with distilled water to remove water soluble impurities and unreacted compounds.

(11) Finally water was removed by washing nanoparticles with acetone.

(12) This acetone –wet slurry was dispersed in 5 ml of engine oil and stirred for 1 hour under mild heating (50 °C) till acetone got evaporated. The resulting fluid was centrifuged at 5000 rpm for 10 min to remove clusters of magnetic particles.

2) Synthesis of water based magnetic fluid

(1) 2.78 gm. of $FeSO_4.7H_2O$ was dissolved in 50 ml water, 5.40 gm. of $FeCl_3.6H_2O$ was dissolved in 50 ml water.

(2) Solution of $FeSO_4$ and $FeCl_3$ were added gradually, dilute HCl was added until pH falls to 1.5.

(3) Solution was stirred for 20 minutes.

(4) Solution was decanted with distilled water.

(5) 14 ml ammonia was dissolved in 86 ml water and mixed with iron sulphate and iron chloride solution. pH was reached up to 10.

(6) Solution was added with ammonium oleate, Stirring was continued for 1 hour and coating of surfactant was carried out by keeping 95^{o}c temperature for 2 minutes.

(7) Then solution was cooled with mechanical stirring. pH value was reached up to less than 5.

(8) The solution was given magnetic decantation 4 times with warm water.

(9) Added ethanol to the solution.

(10) Added acetone to remove precipitates and now solution was transferred to the new beaker, heated and solution was second time coated with oleic acid.

(11) This acetone –wet slurry was dispersed in water and stirred for 1 hour under mild heating (50 °C) till acetone got evaporated.

(12) The resulting fluid was centrifuged at 3000 rpm for 10 min to remove clusters of magnetic particles.

These processes can be explained by the figure no. 3.4 and figure 3.5.

Oil based magnetic fluid

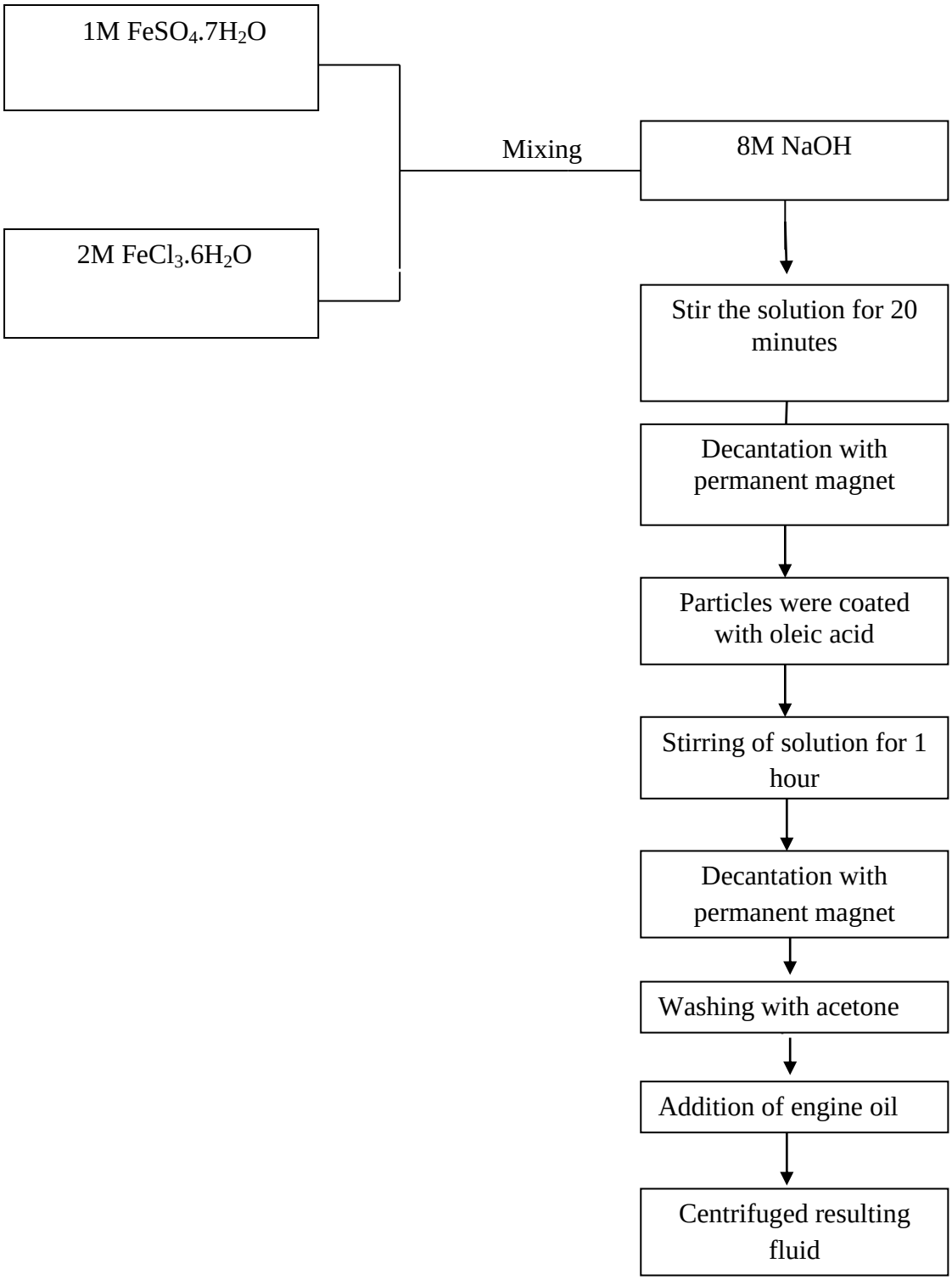

Figure 3.4 Preparation of oil based magnetic fluid

Water based magnetic fluids

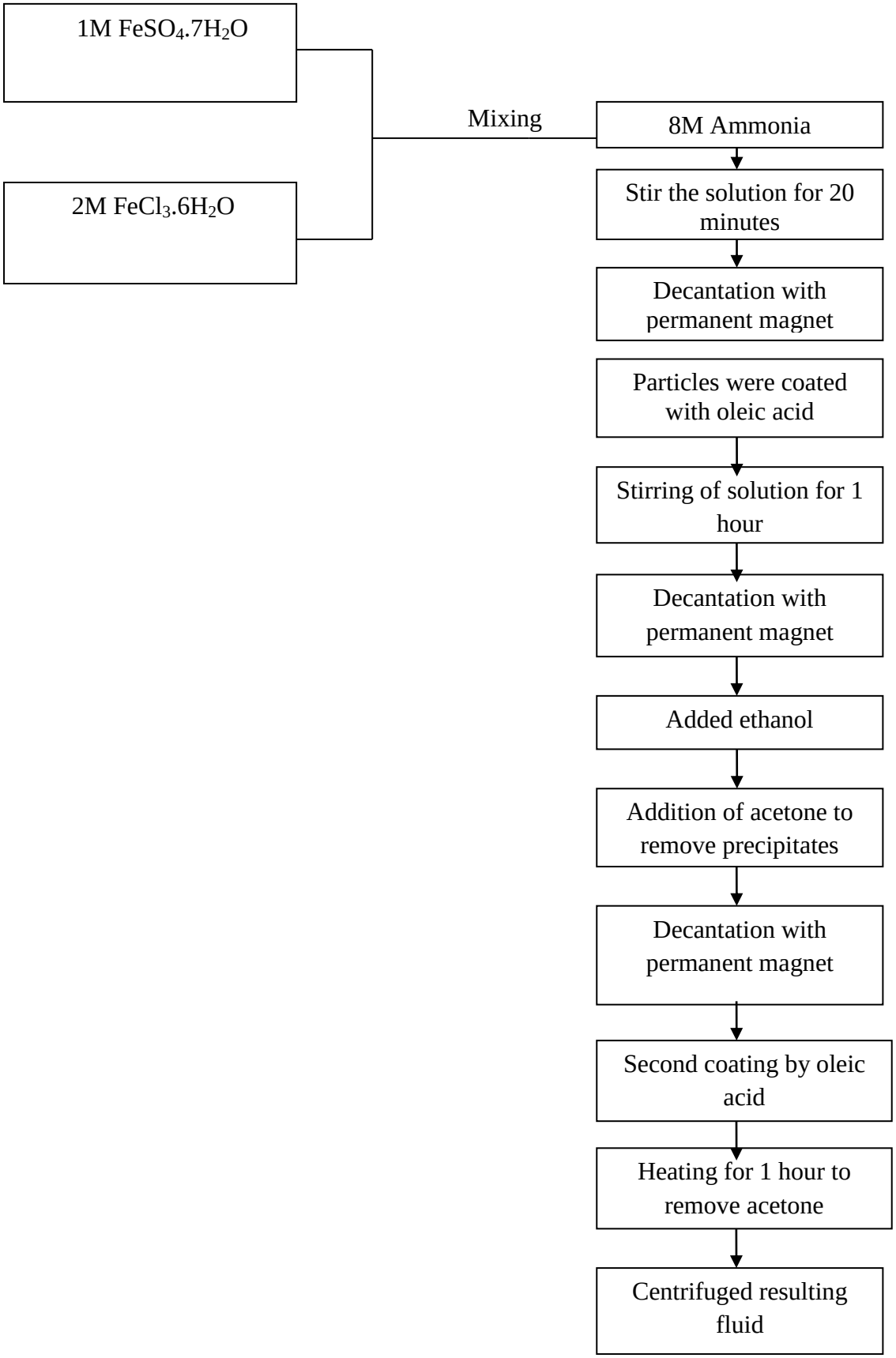

Figure 3.5 preparation of water based magnetic fluid

3.2 Characterization techniques

3.2.1 X-ray diffraction

X-ray diffraction (XRD) is a versatile, non-destructive technique that reveals detailed information about the chemical composition and crystallographic structure of natural and manufactured materials. For diffraction applications, only short wavelength x-rays (hard x-rays) in the range of a few angstroms to 0.1 angstrom (1 keV - 120 keV) are used. Because the wavelength of x-rays is comparable to the size of atoms, XRD spectra is used for determining the crystallographic identity of the produced material, phase purity and calculating the mean particle size on the broadening of the most prominent peak in the XRD profile . Scherer's equation is used to calculate the average particle diameter D (in Å),

$$D = K\lambda/\beta \cos\theta \ldots\ldots \text{ Scherer's equation}$$

where θ is the angle of the peak, β is the width at half maximum (FHWM) of the respective XRD peak, λ is the X-ray radiation wavelength in angstroms (Å) and K is a constant which is very close to unity and is related both to the crystallite shape and to the way in which β and D are defined. The broadening of the diffraction peaks is related to the small particle size .X-rays are produced generally [35] whenever high-speed electrons collide with a metal target, to produce x-ray than the x-ray tube must contain:

1) A source of electrons

2) A high accelerating voltage

3) A metal target

All x-ray tubes contain two electrodes an anode (the metal target) at ground potential, and a cathode maintained at a high negative potential .X-ray tubes may be classify into gas tubes ,in which electrons are produced by the ionization of a small quantity of gas ,and filament tubes in which the source of electrons is a hot filament [36] . In a X-ray tube when a focused electron beam accelerated across a high voltage field bombards a stationary or rotating solid target. As electrons collide with atoms in the target and slow down, a continuous spectrum of x-rays are emitted. The high energy electrons also eject inner shell electrons in atoms through the ionization process. When a free electron fills the shell, an x-ray photon with energy

characteristic of the target material is emitted. Common targets used in x-ray tubes include Cu and Mo, which emits 8 keV and 14 keV, X-rays with corresponding wavelengths of 1.54 Å and 0.8 Å, respectively.

X-rays primarily interact with electrons in atoms. When x-ray photons collide with electrons, some photons from the incident beam will be deflected away from the direction where they originally travel. If the wavelength of these scattered x-rays did not change (meaning that x-ray photons did not lose any energy), the process is called elastic scattering in that only momentum has been transferred in the scattering process. These are the x-rays that we measure in diffraction experiments, as the scattered x-rays carry information about the electron distribution in materials. On the other hand, in the inelastic scattering process, x-rays transfer some of their energy to the electrons and the scattered x-rays will have different wavelength than the incident x-rays. Diffracted waves from different atoms can interfere with each other and the resultant intensity distribution is strongly modulated by this interaction. If the atoms are arranged in a periodic fashion, as in crystals, the diffracted waves will consist of sharp interference maxima (peaks) with the same symmetry as in the distribution of atoms. Measuring the diffraction pattern therefore allows us to deduce the distribution of atoms in a material. The peaks in a x-ray diffraction pattern are directly related to the atomic distances. Let us consider an incident x-ray beam interacting with the atoms arranged in a periodic manner. The atoms, represented as red in the graph, can be viewed as forming different sets of planes in the crystal. For a given set of lattice planes with an inter-plane distance of d, the condition for a diffraction (peak) to occur can be simply written as:

$$2d\sin\theta = n\lambda \quad \text{..... Bragg's law}$$

This is known as the Bragg's law, after W.L. Bragg, who proposed it first. In the equation, λ is the wavelength of the x-ray, θ the scattering angle and n is an integer representing the order of the diffraction peak. The Bragg's Law is one of most important laws used for interpreting x-ray diffraction data.

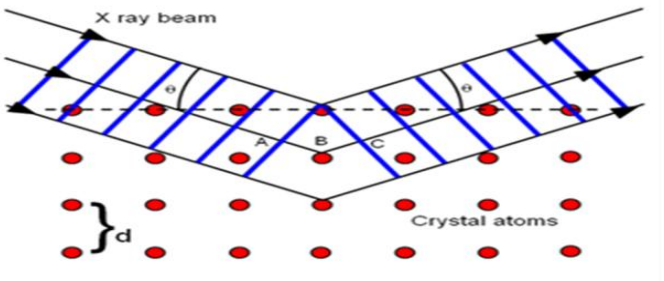

Figure 3.6 Bragg's Law reflection.

3.2.2 Transmission Electron Microscope

Transmission electron microscope is one type of the electron microscopy which is a scientific instruments that use a beam of highly energetic electrons to examine objects on a very fine scale and give information about topography, morphology, composition and crystallographic information .The Transmission electron microscope (TEM) was the first type of electron microscope, it was developed by Max knoll and Ernst Ruska in Germany in 1931. Transmission Electron Microscope (TEM) functions exactly as their optical counterparts except that they use a focused beam of electrons instead of light to image the specimen and gain information as to its structure and composition. The basic steps involved in TEM are:

1) A stream of electrons is formed in high vacuum by electron gun.

2) This stream of electrons are accelerated towards the specimen (with positive electrical potential) while is focused using metal apertures and magnetic lenses into a thin, focused, monochromatic beam.

3) The sample is irradiated by the beam and interactions occur inside the irradiated sample and the interactions inside the sample and effects are detected and transformed into an image [37].

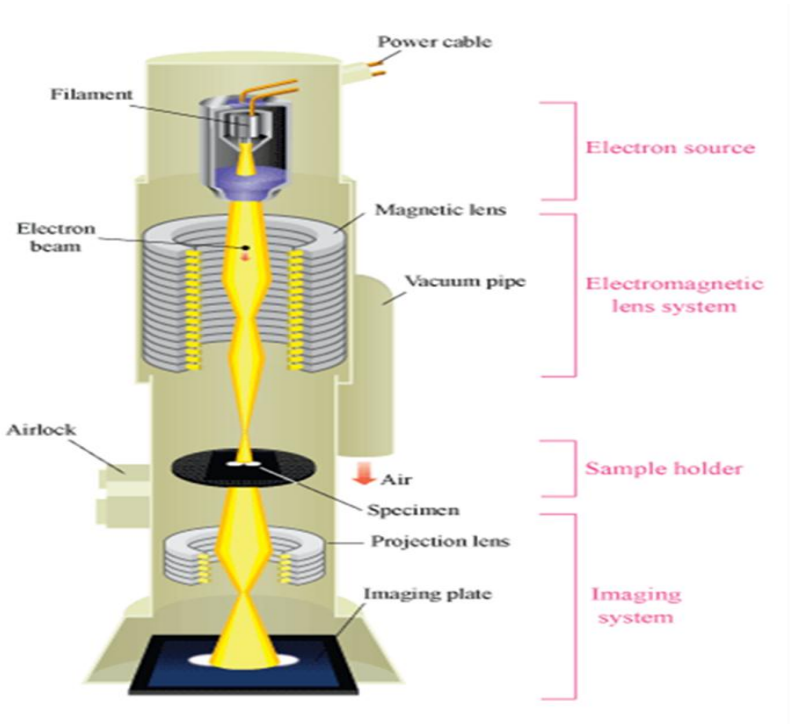

Figure 3.7 The schematic outline of a TEM

TEM show three different interactions between sample and electron beam-specimen:

1) Unscattered electrons (transmitted beam),when incident electrons are transmitted through the thin specimen without any interaction occurring inside the specimen then the beam is called transmitted .Areas of the specimen that are thicker will have fewer transmitted unscattered electrons and so will appear darker, conversely the thinner areas will have more transmitted and thus will appear lighter.

2) Elastically scattered electrons (diffracted beam), incident electrons are scattered by atoms in the specimen in an elastic fashion and these scattered electrons are then transmitted through the remaining portions of the specimen .This pattern can then give information about the orientation , atomic arrangements and phases present in the examined area [38].

3) Inelastically scattered electrons, where incident electrons that interact with specimen atoms in an inelastic fashion, these electrons are then transmitted through the rest of the specimen. Inelastic scattered can give information about elemental composition and atomic bonding state. `

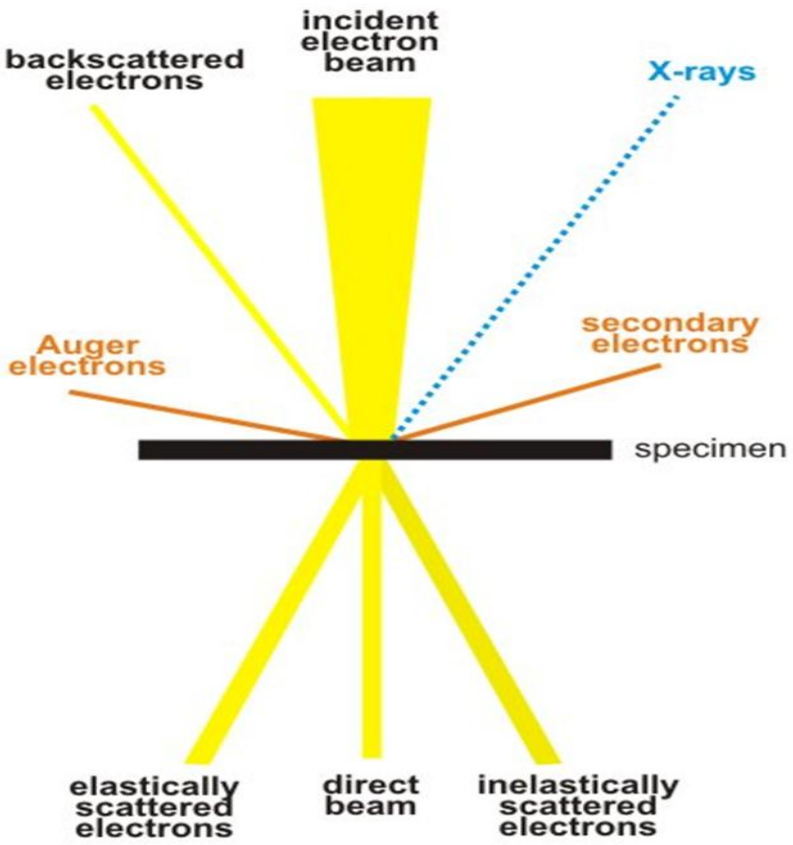

Figure 3.8 Different interactions between sample and electron beam-specimen in TEM [39]

3.2.3 Vibrating Sample Magnetometer

A vibrating sample magnetometer (VSM) is a scientific instrument that measures magnetic properties, invented in 1955 by Simon Foner at Lincoln Laboratory. The vibrating sample magnetometer has become a widely used instrument for determining magnetic properties of a large variety of materials: diamagnetic, paramagnetic, ferromagnetic, ferromagnetic and antiferromagnetic and give information about the hysteresis, saturation, coercivity and anisotropy. Based on Faraday's law of induction, the VSM relies on the detection of the emf induced in a coil of wire. The operation of the VSM is fairly simple. A magnetic sample is placed on a long rod and then driven by a mechanical vibrator. The rod is positioned between the pole pieces of an electromagnet, to which detection coils have been mounted. The oscillatory motion of the magnetized sample will induce a voltage in the detection coils. The induced voltage is proportional to the sample's magnetization, which can be varied by changing the dc magnetic field produced by the electromagnet. When a sample of any material is placed in a uniform magnetic field, created between the poles of a electromagnet, a dipole moment will be induced. If the sample vibrates with sinusoidal motion a sinusoidal electrical signal can be induced in suitable placed pick-up coils. The signal has the same frequency of vibration and its amplitude will be proportional to the magnetic moment, amplitude, and relative position with respect to the pick-up coils system. The sample to be studied is kept in a constant magnetic field. If the sample is magnetic, this constant magnetic field will magnetize the sample by aligning the magnetic domains, or the individual magnetic spins, with the field. The stronger the constant field, the larger the magnetization will be. The magnetic dipole moment of the sample will create a magnetic field around the sample, sometimes called the magnetic stray field. As the sample is moved up and down. This magnetic stray field is changing as a function of time and can be sensed by a set of pick-up coils. The alternating magnetic field will cause an electric current in the pick-up coils according to Faraday's Law of Induction. This current will be proportional to the magnetization of the sample. The greater the magnetization, the greater the induced current. The induction current is amplified by a transimpedance amplifier and lock-in amplifier. The various components are hooked up to a computer interface [40].

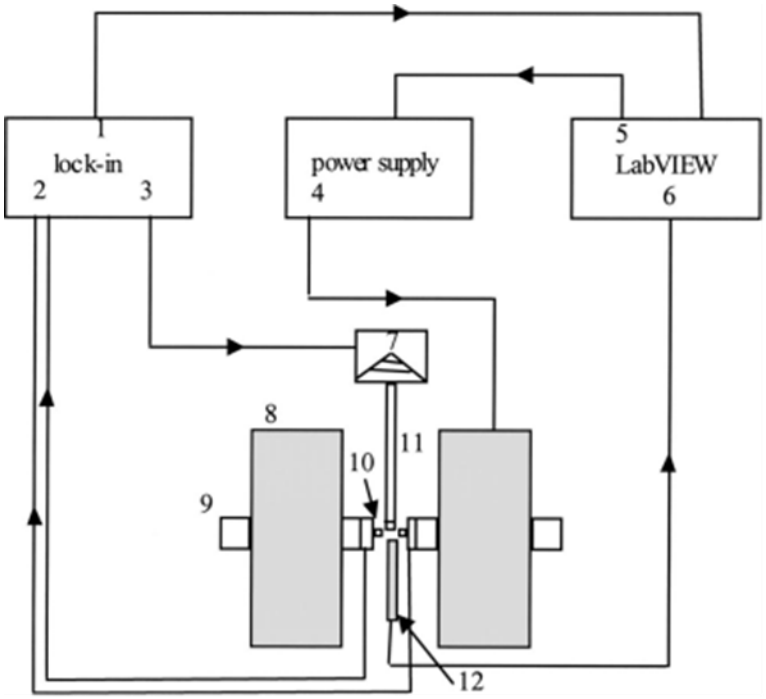

Figure 3.9 Schematic diagram of the VSM apparatus showing:

(1) coil measurement signal path from the lock-in to Lab VIEW via GPIB, (2)signal from the detection coils, (3) driving signal from the lock-in to the mechanical vibrator, (4) the power supply connection to the magnet, (5) the power supply control signal from Lab VIEW, (6) The Hall-probe input to Lab VIEW via the DAC, (7) mechanical vibrator, (8) electromagnet, (9) magnet pole pieces, (10) detection coil, (11) drinking straw shaft, and (12) Hall probe.

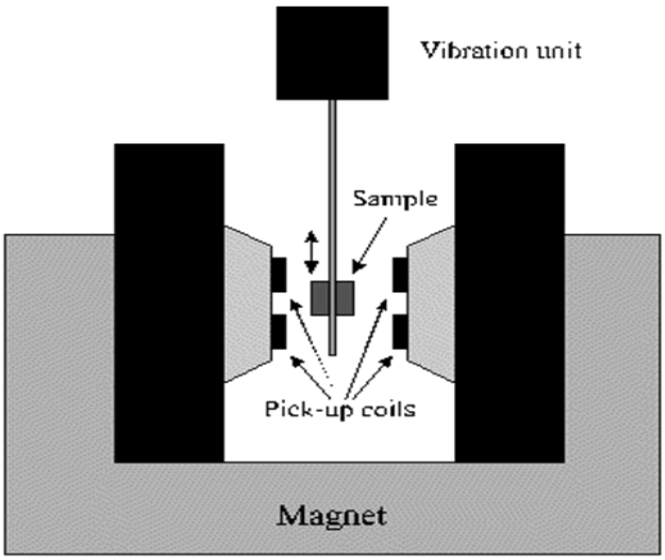

Figure 3.10 Schematic of a VSM. The signal in the pick-up coils is caused by the flux change produced by the moving magnetic sample [41].

Chapter 4

RESULTS AND DISCUSSIONS

Characterization of Fe_3O_4 nanoparticles

In this chapter, we discuss results obtained from X-ray diffraction, Transmission electron Microscopy (TEM) and Magnetization measurements on Vibrating sample Magnetometer (VSM) of Fe_3O_4 nanoparticles.

4.1 TEM Analysis

Transmission electron microscopy images patterns were recorded on JEOL (model GEM 200) transmission electron microscope, which operates at 200 kV. For this purpose, a fine drop of magnetic fluid dispersed in water placed on carbon-coated copper grids and the water was allowed to evaporate slowly at room temperature. TEM image is shown in figure no. 4.1 we can see that particles are nearly spherical and average size is ~14.1 nm. It is clear that there is no agglomeration in the sample. Polydispersity index is 0.2.

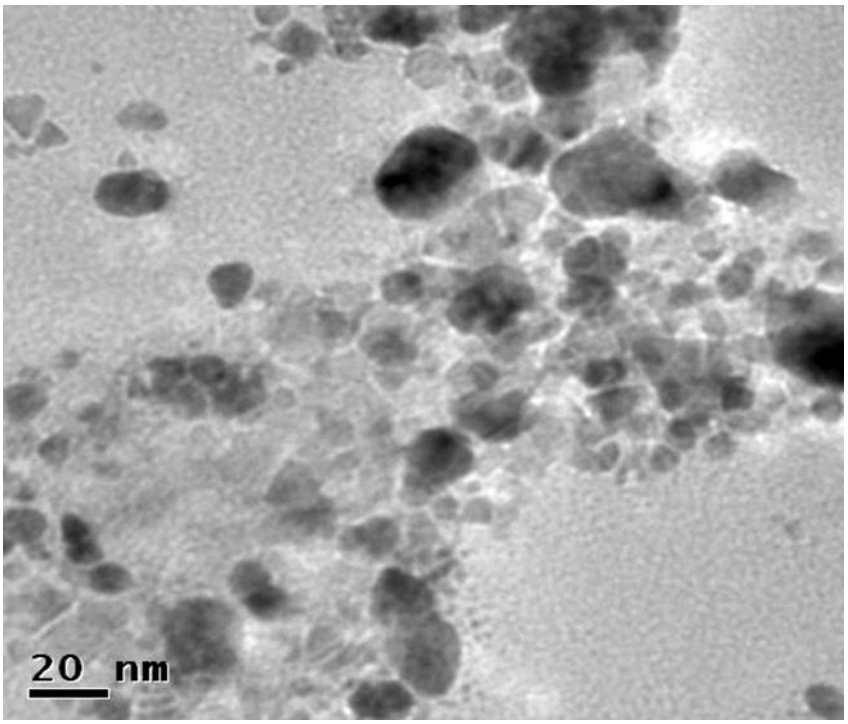

Figure 4.1 TEM image of Fe_3O_4 nanoparticles

4.2 Magnetization Measurements Using VSM

The magnetization measurements were done at room temperature up to a maximum magnetic field (H) of 4000 Oe on vibrating sample magnetometer. From this measurement the saturation magnetization of the fluids were determined.

4.2.1 Oil based magnetic fluids

Figure 4.2 shows the magnetization, M (emu/g), as a function of the applied magnetic field, H (Oe), saturation magnetization (M_s) of the oil based sample is determined from Figure 4.2 and value is listed in Table 1.

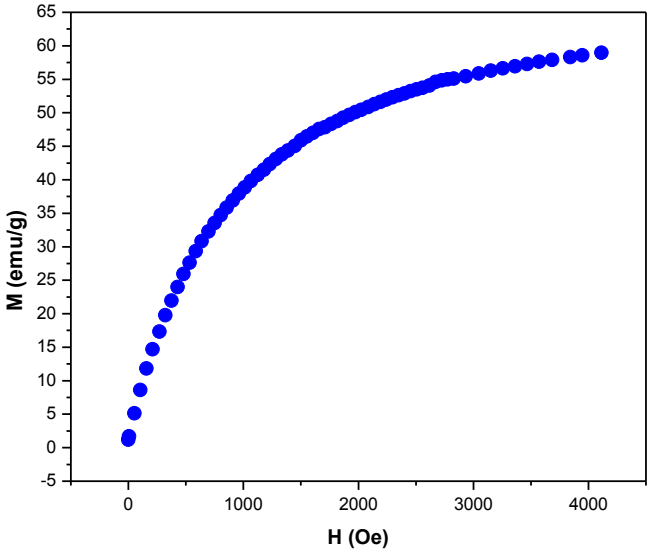

Figure 4.2 Magnetization of Fe_3O_4 nanoparticles as a function of magnetic field (oil based sample)

It can be readily observed that the smaller particle sizes exhibit smaller values of Ms as expected due to the surface disorder and modified cationic distribution [42]. In other words, the decrease in Ms at smaller sizes is attributed to the pronounced surface effects in these nanoparticles. , it is clear that as the magnetic field increases, the magnetization increases and saturates at higher field.

The surface of the nanoparticles is considered to be composed of some canted or disordered spins that prevent the core spins from aligning along the field direction resulting in decrease of the saturation magnetization of the small sized nanoparticles [43].

4.2.2 Water based sample:

From figure 4.3, it is clear that as the magnetic field increases, the magnetization increases and saturates at higher field, but saturation magnetisation is less as compared to oil based sample.

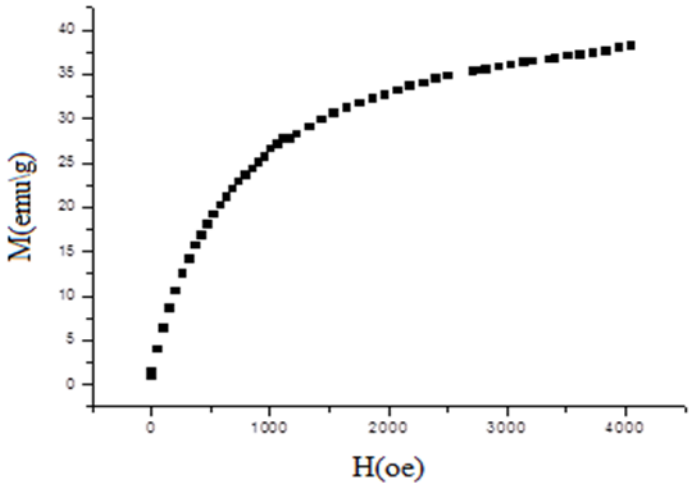

Figure 4.3 Magnetization of Fe_3O_4 nanoparticles as a function of magnetic field (water based sample

Table 1. Magnetic properties of magnetic fluids.

SAMPLE	SATURATION MAGNETIZATION (emu/g)
Sample 1 (Oil based)	38.23
Sample 2 (Water based)	58.65

4.3 XRD Analysis

Structural investigation of magnetite nanoparticles and magnetite nanoparticles were carried out on Bruker D8 Advanced X-ray diffractometer. The X-ray diffraction patterns were recorded at room temperature using monochromatic Cu K_α radiation (k = 1.54056 nm).

X-ray diffraction spectrum of synthesized Fe_3O_4 nanoparticles is shown in Figure 4.4. The peaks positioned at 30.20 °, 35.27 °, 43.22°, 53.690°, 57.230°, 63.480° were index to (220), (311), (400), (422), (511),(440) .crystal planes, respectively. The observed diffraction peaks were corresponding to those of standard pattern of Fe_3O_4 [44] with no extra lines indicating that the samples have single-phase inverse spinel structure and no other phase was present in these samples.

The crystalline size was calculated from the peak broadening of the (311) peak by using by classical Scherrer equation:

$$D = \frac{0.9\,\lambda}{\beta cos\theta B}$$

Where D is crystalline size, λ is wave length of incident x-ray, β is Full Width half Maximum (FWHM) and θ is the half of the diffraction angle of the corresponding peak.

$$\lambda = 1.54 \text{ Å} = 1.54 \times 10\text{-}^{10} \text{ m}$$

FWHM = 0.015689 radians

$$\theta_B = 0.3099 \text{ radians}$$

The corresponding calculated crystallite size was 8.8nm.

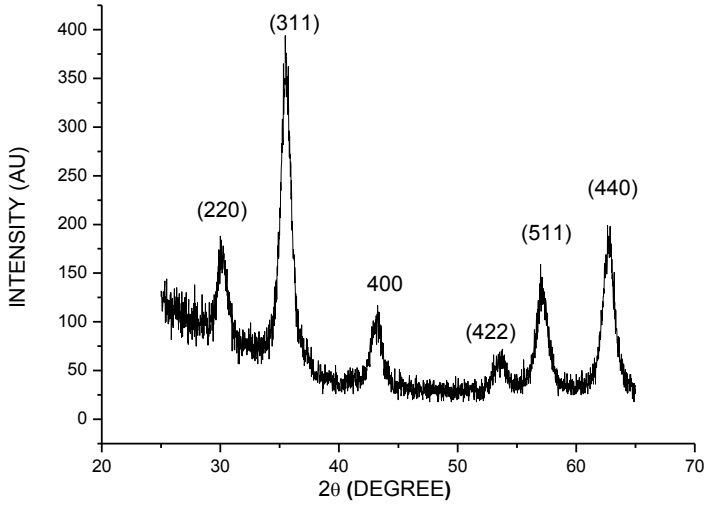

Figure 4.4 XRD patterns of Fe_3O_4 nanoparticles

Table 2 Planes, angles, interplanar spacing and lattice parameter of Fe_3O_4.

(h k l)	2θ(degree)	θ(degree)	d(Å)	a(Å)
(220)	29.88	14.94	2.98	8.40
(311)	35.52	17.76	2.54	8.42
(400)	43.10	21.55	2.09	8.36
(422)	53.61	26.80	1.71	8.37
(511)	57.13	28.56	1.60	8.31
(440)	62.73	31.36	1.47	8.30

4.4 Conclusions

(1) Fe_3O_4 nanoparticles are prepared by co-precipitation method at relatively low temperature.

(2) An x-ray diffraction study indicates that single phase spinel structure nanoparticles are produced with size 8.8 nm.

(3) Coating of oleic acid successfully achieved on nanoparticles and they were dispersed in water and oil to prepare stable magnetic fluids.

(4) TEM analysis indicates that oleic acid coating prevents agglomeration of nanoparticles and average size is 14.1 nm.

(5) VSM analysis reveals that magnetisation increases with increase in applied magnetic field. Saturation magnetisation of oil based sample is more than water based sample.

References

[1] R.E. Rosensweig, Ferrohydrodynamics, 67, 1985, 289-295.

[2] S.Odenbach, Ferrofluids: Magnetically Controllable Fluids and Their Applications, 593D, 2002,250.

[3] S. Odenbach, Colloid Surface, A 217, 2003,171.

[4] W. Zhong, Y. Du, Magnetic Liquids, in: Handbook of Nanophase and Nanostructured Materials, 4, 2002, 96.

[5] B.M. Berkovsky, V.F. Medvedev, M.S. Krakov, Magnetic Fluids Oxford University Press, 1993,164.

[6] C. Scherer and A. M. Figueiredo Neto, Brazilian Journal of Physics, 35, 2005, 718 – 719.

[7] MJ Rosen and JT Kunjappu, Surfactants and Interfacial Phenomena, 4, 2012, 356-358.

[8] R E Rosensweig, Magnetic Fluids Annual Review of Fluid Mechanics 19, 1987, 437-461.

[9] R Patel, Effective viscosity of magnetic nanofluids through capillaries E 85, 2012, 026316.

[10] K. Raj and R. Moskowitz, Commercial applications of ferrofluids, 85, 1990, 233-245.

[11] C. Scherer and A. M. Figueiredo Neto, Ferrofluids: properties and applications,35, 2005,154.

12] C.Scherer and J.A.Miranda, Proceedings of the 10th international conference on magnetic fluids, 289, 2005,484.

[13] A. M. Figueiredo Neto and M. M. F. Saba, Phys. Rev. A 34, 1986, 3483.

[14] A. S. Lübbe, C. Alexiou, and C. Bergemann, Clinical Applications of Magnetic Drug Targeting, 35, 2005 718 - 719.

[15] Q.A. Pankhurst, J. Connolly, S.K. Jones, and J.Dobson, Applications of magnetic nanoparticles in biomedicine, R167, 2003, 36.

[16] R Moskowitz and Hollis, Magnetic fluids – cooled electromagnetic device and improved cooling method, 685, 1995, 5462.

[17] T. Cader, B.A. Finlayson, Finite element model of magneto convection of a ferrofluid, 262, 2003, 269-279.

[18] W Yuan , C Yin ,P Xiao, X Wang ,J Sun , S Huang , Microsecond-scale switching time of magnetic fluids due to the optical trapping effect in waveguide structure, 11,2011, 781–785.

[19] V. M. Chakka, B. Altuncevahir, Z. Q. Jin, Y. Li, and J. P. Liua, Magnetic nanoparticles produced by surfactant-assisted ball milling, 99, 2006, 08e912.

[20] S Xuan, Preparation of water-soluble magnetite nanocrystals through hydrothermal approach, 308, 2007, 210–213.

[21] N. N. Nassar , Preparation Of Iron Oxide Nanoparticles From $FeCl_3$ Solid Powder Using Microemulsion ,6, 2006,1324-1328.

[22] Hassan Karami, Synthesis and Characterization of Iron Oxide Nanoparticles by Solid State Chemical Reaction Method, 21, 2010, 11–20.

[23] Nguyen Thai Ha, Effects of the conditions of the microemulsion preparation on the properties of Fe_3O_4 nanoparticles, 24, 2008, 9-15.

[24] D.Maity, Synthesis of iron oxide nanoparticles under oxidizing environment and their stabilization in aqueous and non-aqueous media, 308 ,2007, 46–55.

[25] W. Voit, D.K. Kim ,W. Zapka, M. Muhammed , and K.V. Rao Magnetic behavior of coated superparamagnetic iron oxide nanoparticles in ferrofluids, 676 ,2001, Y7.8.1- Y7.8.7.

[26] M. Kawashita, Effect of Particle Size of Magnetite Nanoparticles on Heat Generating, 1, 2011, 1-4.

[27] Maity, Synthesis of magnetite nanoparticles via a solvent-free thermal decomposition route, 321, 2009, 1256-1259.

[28] S Fun Chin "Green Synthesis of Magnetite Nanoparticles (via Thermal Decomposition Method) with Controllable Size and Shape, 2 (3), 2011, 299-302.

[29] M. I. Florez -Zamora, Comparative study of Al-Ni-Mo alloys obtained by mechanical alloying in different ball mills,. 18, 2008,301.

[30] R.S Ellis, Wagner, W.C, Vapor-liquid-solid mechanism of single crystal growth, 5, 1964,210.

[31] Lu, Yicheng, Zhong, Jian, Todd Steiner, Semiconductor Nanostructures for Optoelectronic Applications 5, 2004,191–192.

[32] Ab Brinker, C.J.; G.W. Scherer, Sol-Gel Science: The Physics and Chemistry of Sol-Gel Processing. Academic Press. ISBN 0-12-134970-5,1990.

[33] L.L.; J.K. West, Hench, the Sol-Gel Process, 1, 1990, 33.

[34] R.V.Mehta and R.V Upadhyay, 76, 1999, 305 – 312.

[35] Patnaik, P. Dean's Analytical Chemistry Handbook, 2nd ed. McGraw-Hill, 2004.

[36] B.D.Cullity, S.R.Stock. Elements of x-ray Diffraction, Prentice Hall,2001.

[37] M. Faraji, Y. Yamini and M. Rezaee, Magnetic Nanoparticles Synthesis, Stabilization, Functionalization, Characterization, and Applications, 7, 2010, 1-37.

[38] D B.Williams, C.Barry Carter, Transmission Electron Microscopy. Plenum Publishing Corporation.

[39] http://www.hk-phy.org/atomic_world/tem/tem02_e.html [accessed 29/5/2012]

[40] Wesley Burgei, Michael J. Pechan, and Herbert Jaeger. A simple vibrating sample magnetometer for use in a materials physics course. Department of Physics, Miami University, Am. J. Phys. 71 (8), August 2003.

[41] http://www.el.utwente.nl/tdm/istg/research/vsm/vsm.htm [accessed 29/5/2012]

[42] L. Victoria, Calero, Carlos, J Rinaldi, Magnetic matter 314 (2007) 60.

[43] H.E Ghandoor1, H. M. Zidan, Mostafa M.H. Khalil and M. I. M. Ismail, Synthesis and Some Physical Properties of Magnetite (Fe_3O_4), 7 (2012) 5734 – 574.

[44] N Andhariya, B Chudasama, R. V. Mehta, R. V. Upadhyay, Nano engineering of methylene blue loaded silica encapsulated magnetite nanospheres and nanocapsules for photodynamic therapy, 13, 2011, 3619–3631